Nanometric Inhomogeneity of Polymer Network Investigated by Scanning Near-Field Optical Microscopy

Hiroyuki Aoki, Shigeyuki Tanaka, and Shinzaburo Ito*

Department of Polymer Chemistry, Graduate School of Engineering, Kyoto University, Sakyo-ku, Kyoto 606-8501, Japan

Masahide Yamamoto

Section of Applied Chemistry, Faculty of Science and Engineering, Ritsumeikan University, Kusatsu City, Shiga 520-8577, Japan

Received July 20, 2000

ABSTRACT: The structural inhomogeneity of the poly(methyl methacrylate) (PMMA) network was studied by scanning near-field optical microscopy (SNOM), which provides us optical images and spectroscopic information in a local area with a spatial resolution of several tens of nanometers. The optically transparent PMMA network was labeled with fluorescent dyes either at the network chain or at the cross-linking points. The spatial distribution of the chain segments and cross-links could be directly visualized in real space, and the PMMA network was found to have an inhomogeneous structure in a scale of submicrons. Nanosecond dynamics of the energy transfer among the dyes introduced to the side chain was also examined in a nanometric area by the time-correlated photon counting system combined with SNOM. The fluorescence decay through the near-field excitation showed that the local segment density was ca. 10 times higher than the ensemble average density. The local segment density had little correlation with the structure in a submicron scale observed by SNOM. These findings indicated that the PMMA network has structural hierarchy.

Introduction

Gels, which consist of three-dimensional networks of polymer chains, have attracted much attention for a long time from the viewpoints of both fundamental physical chemistry and applications to various fields. Since the structural heterogeneity is a critical factor for determining the functions of gels, the internal structure of polymer networks has been extensively investigated by many workers.[1−13] In a gelation process, the fluctuations of polymer density are frozen permanently by the introduction of cross-linking, resulting in the static structural inhomogeneity.[5] The heterogeneity of the network structure has been found to increase with the increase of cross-link density.[4,6] Recently, Shibayama et al. demonstrated the inverse dependence on the cross-link density in weakly charged hydrogels in particular experimental conditions, such as the temperature and the degree of ionization.[7−9] They explained the inverse phenomenon on the basis of Rabin−Panyukov theory.[10]

Although the inhomogeneity of the polymer networks has been mainly studied by various scattering techniques, few direct observations in real space have been reported. Suzuki et al. investigated the surface structure of poly(acrylamide) (PAAm) and poly(*N*-isopropylacrylamide) (PNIPAm) gels by atomic force microscopy.[11,12] They showed that the submicron structure of the gel surface was strongly dependent on the cross-link density and the osmotic pressure. Hirokawa et al. examined the three-dimensional internal structure of the PNIPAm gels in a scale of several microns using a confocal microscope.[13] They discussed the preparation temperature dependence of the internal structure and showed that the gels had a bicontinuous structure of dense and sparse regions in the PNIPAm gel.

Fluorescence techniques have been widely used for investigation of structure and dynamics of various polymer systems,[14−19] and it seems to be also useful to study the internal structure of polymer networks. However, the fluorescence techniques have not been applicable to the local area smaller than several hundred nanometers because of the diffraction limit of light for the conventional optical microscopy. Scanning near-field optical microscopy (SNOM), which has been developed recently, allows one to take optical micrographs and spectroscopic information in a nanometric local area where the specimen is illuminated by the optical near-field emanating from an aperture much smaller than the wavelength of light.[20−27] Because the probe−sample gap is kept constant during the raster-scanning of the sample, the height profile of the sample surface can be obtained simultaneously with the optical image and the spectroscopic properties in the local area with a spatial resolution beyond the diffraction limit. In this study, the static structural inhomogeneity of the poly(methyl methacrylate) (PMMA) network was investigated by means of SNOM. The spatial distribution of the network chain segments labeled with fluorescent groups was directly observed with a resolution of <100 nm. The time-resolved measurements were also carried out by SNOM. The energy transfer among the dyes introduced into the network chain was also discussed in terms of the segment density on the molecular scale.

Experiments

Materials. Figure 1 shows the chemical structures of the PMMA network labeled at the side chains and the cross-linking points. 3-Perylenylmethyl methacrylate was synthesized by the following procedure. 3-Perylenemethanol was synthesized by the reduction of 3-formylperylene, which was

* To whom correspondence should be addressed. Phone +81-75-753-5612, Fax +81-75-753-5632, E-mail sito@polym.kyoto-u.ac.jp.

10.1021/ma001274+ CCC: $19.00
Published on Web 12/01/2000

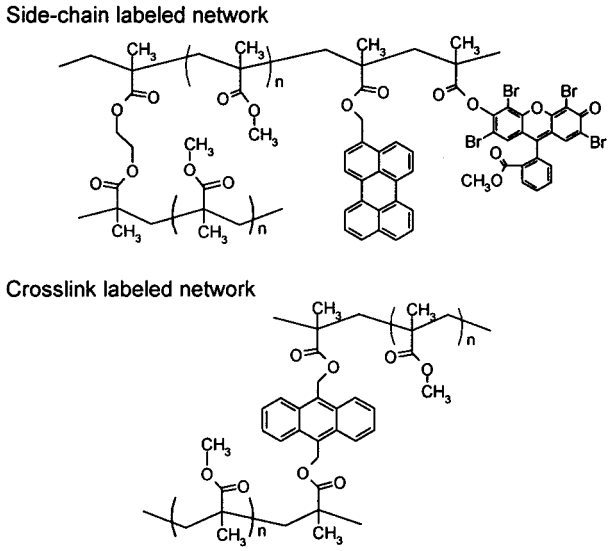

Figure 1. Chemical structure of side-chain and cross-link labeled PMMA network samples.

prepared by Vilsmeiyer reaction of perylene. The esterification of 3-perylenemethanol with methacryloyl chloride (Tokyo Chemical Industry) yielded 3-perylenylmethyl methacrylate, which was purified by column chromatography on silica gel. Eosin-labeled methacrylate monomer was synthesized by the esterification of methacryloyl chloride with methyleosin (Aldrich) and purified through a silica gel column. 9,10-Anthrylenemethyl dimethacrylate was synthesized as a fluorescent cross-linking agent.[16,28]

The PMMA network labeled with perylene at the side chains was prepared by the free radical copolymerization of methyl methacrylate (MMA; Wako Pure Chemical Industries), 3-perylenylmethyl methacrylate (dye-labeled monomer), and ethylene glycol dimethacrylate (cross-linker; Wako Pure Chemical Industries). The cross-link density, which was defined as the molar ratio of cross-linker to the MMA monomer, was varied from 0.1 to 0.5%. *N*,*N*′-Dimethylformamide (DMF), benzene, and acetonitrile were used as solvents. MMA and the solvents were purified by distillation, and ethylene glycol dimethacrylate was used as received. Polymerization was carried out at 60 °C for 15 h in a solution of the monomer mixture (50 vol %) using α,α′-azobis(isobutyronitrile) (Nacalai Tesque) as an initiator. The gels labeled with both perylene and eosin were also prepared similarly. The cross-link labeled network was prepared from MMA and 9,10-anthrylenemethyl dimethacrylate (dye-labeled cross-linker) in a benzene solution with a cross-link density of 0.1%. Polymerization was carried out in the same manner as the case of the side-chain labeled gel. The residual monomer and sol fraction were extracted in distilled toluene until the absorption of the dye was not detected from the decanted solvent. The amount of the extracted dye was determined by UV−vis absorption measurement. The dye-labeled linear PMMA was also prepared according to the same procedure except for the absence of the cross-linker. In SNOM measurement, the samples must be sufficiently thin with respect to the dimension of the expected structure. However, since the gels swollen in a solvent were so fragile that they could not be cut to a thickness of a few hundred nanometers, the sample gels were solidified according to the following procedure. The gels were cut into a thick disk, dried in a vacuum, swollen in MMA, and then heated in order to polymerize the MMA monomer. The resulting network in the PMMA bulk was optically transparent and appeared homogeneous. The gel was sliced to ca. 100 nm thick using an ultramicrotome, and each sample piece was transferred onto a glass coverslip for SNOM measurements.

SNOM Measurements. The SNOM system used in this study was based on a commercially available instrument (SP-301, Unisoku). A block diagram of the SNOM is shown in Figure 2. A CW He−Cd laser (λ = 442 nm; IK5351R-D,

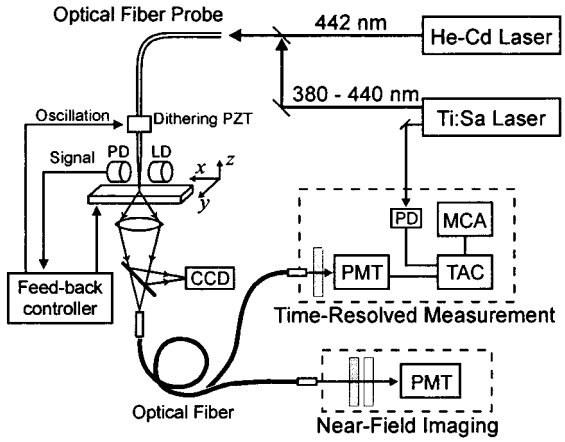

Figure 2. Block diagram of the SNOM system. The SNOM was operated in the illumination mode, and the fluorescence photons from the sample were collected by a microscope objective and guided to a detector through a multimode optical fiber. PD, a photodiode; LD, a laser diode; PMT, a photomultiplier; MCA, a multichannel analyzer; TAC, a time-to-amplitude converter.

Kimmon Electric) and the second harmonic of a picosecond Ti:sapphire laser (Tsunami, Spectra Physics) were used as the light sources. The wavelength of the Ti:Sa laser was 397 and 415 nm for the samples labeled with anthracence and perylene, respectively, and the repetition rate of the excitation pulse was 4 MHz. Homemade SNOM probes were used,[22,29,30] and the diameter of the aperture at the end of a probe was typically 50−100 nm. The distance between the probe and the sample surface was regulated to be several nanometers by a shear force feedback system. The fluorescence from the sample was collected with a high NA objective (1.3 NA, Nikon) and detected with a photomultiplier (R4220P, Hamamatsu Photonics). The obtained SNOM images consisted of 256 × 256 pixels, and the gate time for photon counting was 16 ms for each pixel. The near-field time-resolved measurement was carried out by the time-correlated single photon counting technique.[31] The fluorescence photon signal from the sample and the excitation pulse were fed into a time-to-amplitude converter (TAC; model 457, Ortec). The time-correlated TAC signals were accumulated at a multichannel analyzer (Ino-Tech 5300, Norland) and transferred to a personal computer (PC-9801, NEC). The fwhm of the instrumental response function was ca. 500 ps.

Results and Discussion

Parts a, b, and c of Figure 3 show the topographic, transmission, and fluorescence SNOM images for the same area of the PMMA network side-chain labeled with perylene in which the cross-link density was 0.1%, respectively. In the topographic image (Figure 3a), there were several ridges in an oblique direction. They were "knife marks" on the surface, which were the traces of the glass knife of the microtome due to the roughness of the knife blade. The transmission SNOM image was obtained by recording the intensity of light transmitted through the sample. The contrast in the transmission SNOM image results from the surface topography and the optical properties, such as refractive index and transmittance, beneath the sample surface.[25,32] No structural features besides the knife marks were seen in Figure 3b, indicating that the contrast in this image was mainly affected by the surface topography for the specimen and the internal structure could not be measured. On the other hand, the fluorescence SNOM image (Figure 3c) had no correlation with the topographic image. It can be safely said that the structure seen in Figure 3c is free from the artifact due to the

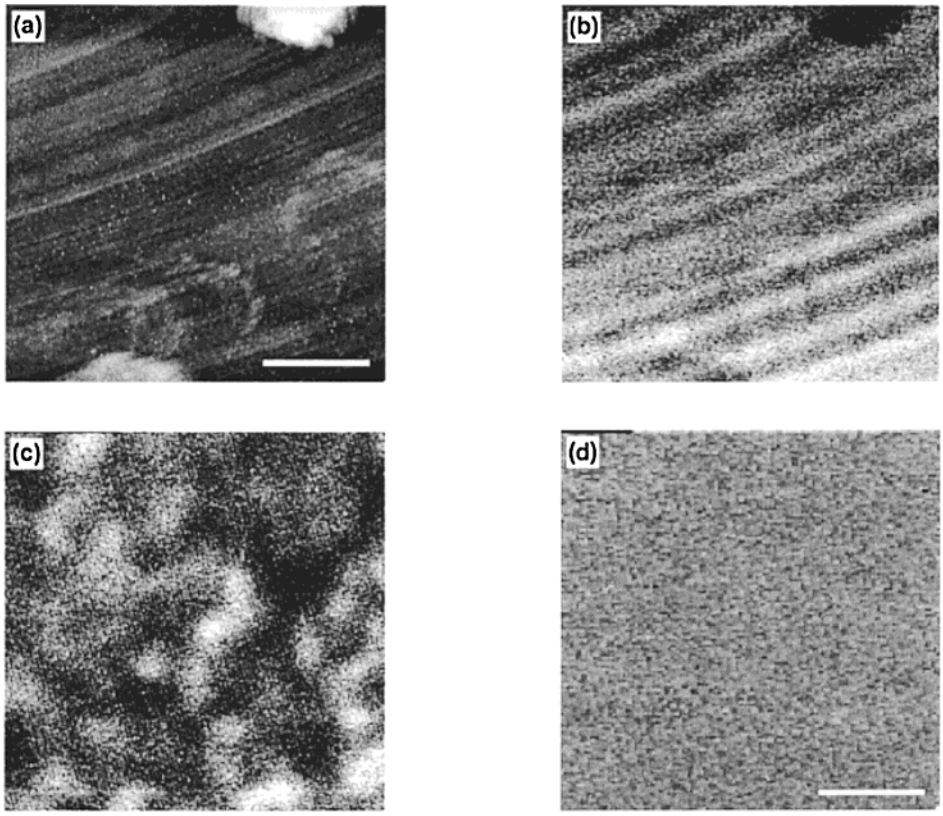

Figure 3. Topographic (a), transmission (b), and fluorescence SNOM images (c) for the PMMA network with a cross-link density of 0.1% and fluorescence image for the un-cross-linked PMMA (d). (a)−(c) were obtained for the same area. The scale bars indicate 1 μm. The wavelength of the light source was 442 nm.

topographic effect at the surface and shows the spatial distribution of the fluorescent dye molecules in the PMMA gel. Thus, the fluorescence SNOM allowed the direct observation of the distribution of the chain segments with a lateral resolution of 100 nm. The PMMA network had structural inhomogeneity in a scale of several hundred nanometers. The topographic images for all the samples were also measured for the larger scanning area to estimate the sample thickness, which was defined as the height difference between the upper surface of the sample and the glass substrate (the images are not shown here). The thickness of each sample was typically 100 nm, which was sufficiently small compared to the dimension of the network structure. As the control experiment, the SNOM measurement was carried out also for the un-cross-linked PMMA sample, which was prepared by the solidification of the dye-labeled linear PMMA dissolved in MMA. Figure 3d shows the fluorescence SNOM image for the un-cross-linked sample. Any contrast could not be seen in Figure 3d. This indicates that the inhomogeneous structure observed in the fluorescence SNOM image (Figure 3c) was not formed by the solidification procedure following the gel preparation but induced by the introduction of cross-linking. Thus, the internal structure of the gel could be successfully measured in a length scale of 100 nm.

Figure 4 depicts the fluorescence SNOM images for the side-chain and cross-link labeled networks, both of which were prepared under the same conditions except for the dye-labeled position. The dimensions of the structure for both samples were estimated to be 500−600 nm, implying that the spatial distribution of the cross-linking points was similar to that of the network chain segments.

The preparation condition, such as temperature and solvent, plays an important role in the formation of polymer network structure. Shibayama et al. reported that the structural inhomogeneity of PAAm and PNIPAm gels was dependent upon the solvent quality in the network formation.[6,8] Figure 5 shows an example of the SNOM images for the PMMA network prepared in acetonitrile, which is a Θ solvent for PMMA. The size of the bright domain was evaluated to be 1 μm, which was much larger than that for the network prepared in benzene. The details are still unclear, but the lower solvent quality may have caused the larger structure, possibly resulting from the aggregation of the chain segments enhanced by phase separation during the network formation.

Figure 6 shows the fluorescence images for the side-chain-labeled network samples with different cross-link densities. It should be noted that it is impossible to compare the absolute values of the fluorescence intensity among the different samples because the excitation intensity and the detection efficiency are not exactly the same for each sample in the near-field experiment. The bright domains were estimated to be ca. 600 and 250 nm for 0.1% and 0.2% samples, respectively. No contrast could be seen in the fluorescence images for 0.3% and higher cross-link densities because the inhomogeneous structure for them was much smaller than the resolution of the SNOM, $\leq$100 nm. The characteristic size of the structure decreased markedly with an increase of the cross-link density. In the gelation process, the cross-links are thought to be introduced heterogeneously because of the concentration fluctuation in the polymerization solution, and then the chain length between cross-linking points had a wide dispersion. Considering the cross-link density of 0.1−0.2%, the size of the

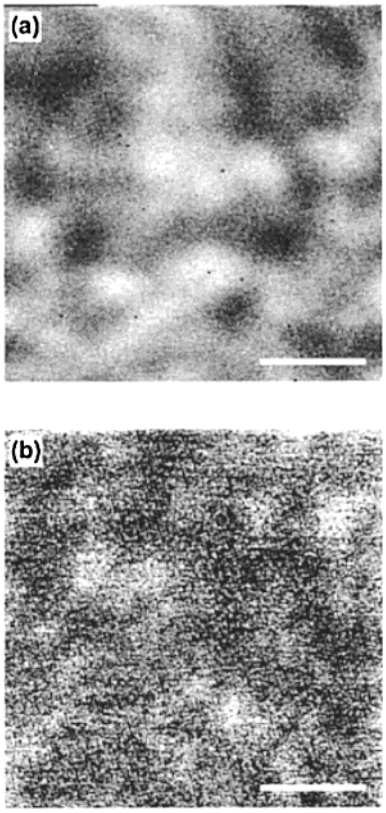

Figure 4. Fluorescence SNOM images for the side-chain (a) and cross-link (b) labeled PMMA networks. The cross-link density was 0.1% for each network. The He−Cd laser (442 nm) and the second harmonic of the Ti:sapphire laser (397 nm) were used as the excitation sources for the side-chain and cross-link labeled samples, respectively. The scale bar in each image indicates 1 μm.

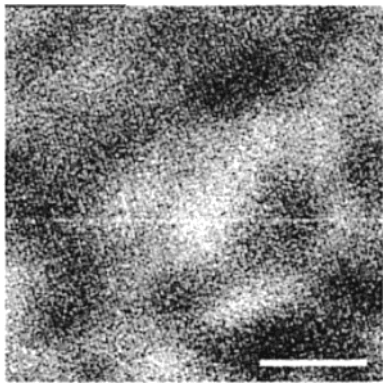

Figure 5. Fluorescence SNOM images for the PMMA network samples prepared in acetonitrile. The cross-link density was 0.1%. The scale bar in each image indicates 1 μm.

structure induced by such a mechanism is expected to be on a scale of ∼10 nm, whereas the domain size measured by SNOM was on a submicron scale. Therefore, the structure imaged by SNOM was not the mesh of the "polymer chain". At the early stage of polymerization, microclusters of polymer chains are formed by introduction of cross-linking. As the polymerization proceeds, the microclusters are cross-linked to each other and form a three-dimensional network. The inhomogeneity of the polymer network on a scale of several hundred nanometers was composed of such a cross-linked microcluster, which is discussed later. For the network with a low cross-link density, intercluster cross-linking occurred after the individual cluster fully

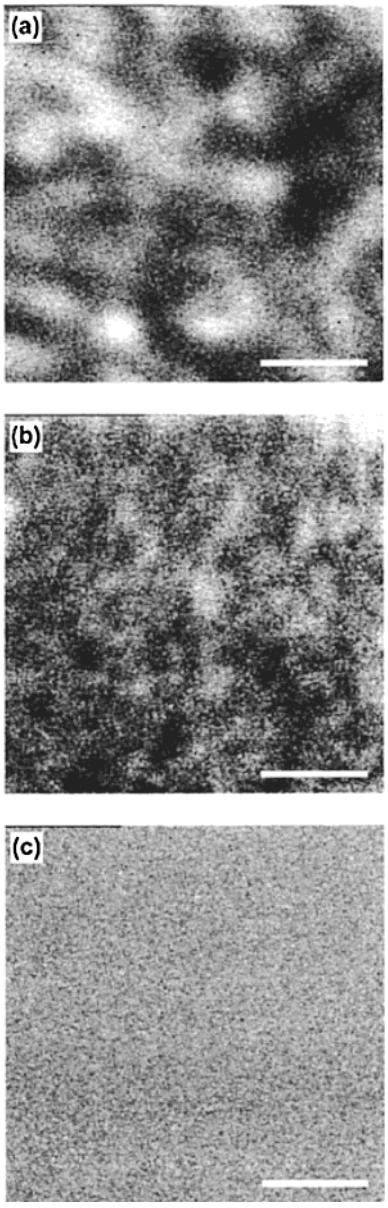

Figure 6. Fluorescence SNOM images for the network samples with different cross-link densities: 0.1% (a), 0.2% (b), and 0.3% (c). The scale bar in each image indicates 1 μm.

increased in size, consequently resulting in a larger domain size. In addition, the polymer chains, which were not incorporated into the infinite polymer network, were also produced in the gel as the sol fraction. They were extracted in the process of the sample preparation, yielding void of polymer segments in the resulting network. Thus, the low cross-link density resulted in a large network structure. On the other hand, the larger cross-link density resulted in a faster and smaller cluster formation, consequently yielding the smaller characteristic size of the network, which appeared more homogeneous under the SNOM images.

The inhomogeneous structure of the PMMA networks on a 100 nm scale could be directly measured by the fluorescence SNOM. Although the knowledge of the structure on the molecular scale is indispensable for understanding the morphology of polymer networks, the lateral resolution of a SNOM micrograph was far from the atomic resolution. Therefore, we investigated the structural inhomogeneity in a nanometer scale by the energy transfer method, which was applied to a local

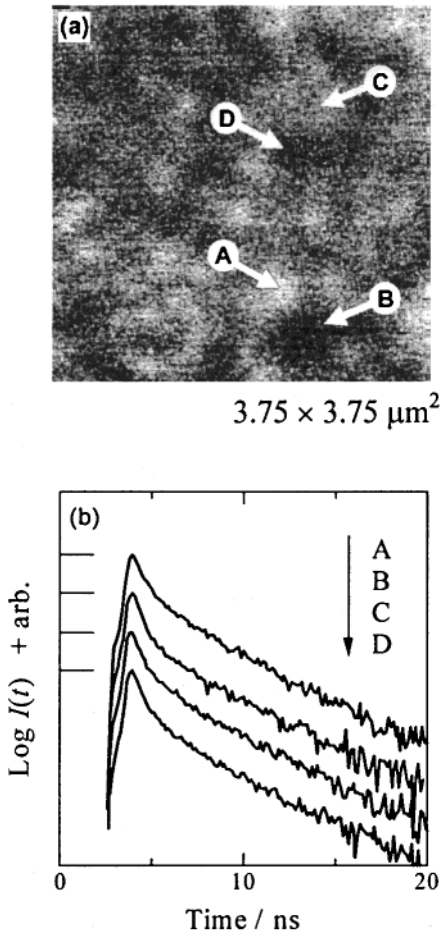

Figure 7. Fluorescence SNOM image (a) and perylene fluorescence decay curves (b) for the PMMA network labeled at side chains with perylene and eosin. The sample was prepared in DMF, and the cross-link density was 0.1%. (a) was obtained by collecting the perylene fluorescence. The scanning area in (a) was 3.75 × 3.75 μm^2. The fluorescence decay in (b) was measured at various points denoted as A, B, C, and D in (a). The excitation wavelength was 415 nm.

area using SNOM. In the sample labeled with both perylene and eosin, the nonradiative excitation energy transfer from perylene (energy donor) to eosin (energy acceptor) occurs when they are close to each other. The rate of the energy transfer by the Förster mechanism is proportional to $(R/R_0)^{-6}$, where R is the distance between a perylene and an eosin molecule and R_0 is the Förster radius. R_0 was determined to be 4.0 nm through a separate experiment; the theoretical decay curves[33] were fitted to the experimentally obtained decays for the PMMA cast films where perylene and eosin were homogeneously dispersed at given concentrations. Therefore, the fluorescence decay of a perylene molecule probes the distance of separation between a perylene and the surrounding eosin molecules in a range of 2−10 nm. The denser the polymer segments are, the faster the fluorescence decays because of the shorter distance to the acceptor. The energy transfer dynamics from perylene to eosin was examined in order to estimate the segment density in the local area by the near-field time-correlated single photon counting technique. Figure 7a shows the perylene fluorescence image for the PMMA network with a cross-link density of 0.1%. The excitation source was a frequency-doubled Ti:sapphire laser operated at 415 nm. Figure 7b depicts the fluorescence decay curves for perylene emission obtained at the points denoted as A, B, C, and D in Figure 7a. The decay profile was fairly similar at all points. Since the energy transfer dynamics is determined by the dye distribution in the distances of 2−10 nm, this implies that the spatial distribution of the network chain at the different points is quite similar within the scale of 10 nm, whereas the network structure is obviously inhomogeneous on the 100 nm scale.

Before discussing the fluorescence decay in more detail, we estimated the concentration of eosin averaged over the whole sample volume, $[\mathrm{Eo}]_{\mathrm{ensemble}}$, assuming that the dye molecules were homogeneously dispersed in the network. $[\mathrm{Eo}]_{\mathrm{ensemble}}$ could be calculated as

$$[\mathrm{Eo}]_{\mathrm{ensemble}} = \frac{N_0 - N_{\mathrm{ext}}}{V_0} \Big/ \left(\frac{d}{d_0}\right)^3 \qquad (1)$$

where N_0, V_0, and d/d_0 are the amount of eosin in feed, the initial volume (just after the polymerization), and the swelling ratio defined as the ratio of the diameters of the network sample in the initial and final states, respectively. The amount of extracted eosin, N_{ext}, was evaluated by UV−vis absorption measurements. The ensemble average concentration, $[\mathrm{Eo}]_{\mathrm{ensemble}}$, for the PMMA network shown in Figure 7 was estimated to be 0.71 mM. The perylene fluorescence decays indicated in Figure 7b were compared to that for the homogeneous system, which was a mixture of perylene and eosin monomer compounds dispersed in a PMMA spin-cast film.[34] The near-field fluorescence decay profiles measured at different points for the spin-cast film were in exact agreement with each other, and the far-field fluorescence decays separately obtained could be well fitted to the theoretical curve for the randomly distributed perylene and eosin molecules in a three-dimensional space:

$$I(t) = I_0 \exp\left(-\frac{t}{\tau_0} - \frac{4}{3}\pi^{3/2} R_0^{\,3} [\mathrm{A}] \left(\frac{t}{\tau_0}\right)^{1/2}\right) \qquad (2)$$

where I_0, [A], and τ_0 are the fluorescence intensity at $t = 0$, the concentration of the acceptor (eosin), and the intrinsic fluorescence lifetime of the donor (perylene) without the energy transfer process, respectively.[33] Thus, the dye-doped spin-cast film can be used as a homogeneous model system.

Figure 8 shows the fluorescence decays for the uncross-linked polymer sample and the spin-cast film, in which the eosin concentrations were 0.70 mM. The decay curve for the network, which is shown as curve A in Figure 7b, is also shown in this figure. Although the averaged dye concentrations were the same for them (0.7 mM), the fluorescence decay profile for the network was quite different from those for the monomer model and linear polymer systems; that is, the decay rate for the network was much larger than those for the homogeneous systems. The initial decay rate corresponded to that for a spin-cast film with [Eo] = 15 mM. It is difficult to simply compare the near-field fluorescence decays because the metal coating of the SNOM probe may affect the fluorescence lifetime.[35−37] However, in our case, both fluorescence decay profiles obtained in the near-field and the far-field were similar for the spin-cast films, implying that the SNOM tip had little influence on the near-field time-resolved measurements. Therefore, it is safely said that the eosin concentration was more than 10 mM; i.e., the chain segment density

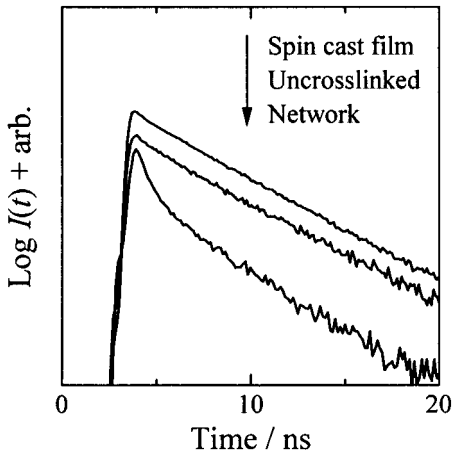

Figure 8. Near-field fluorescence decay curves for the spin-cast film, the un-cross-linked sample, and the polymer network sample. The average eosin concentration for each sample was 0.7 mM.

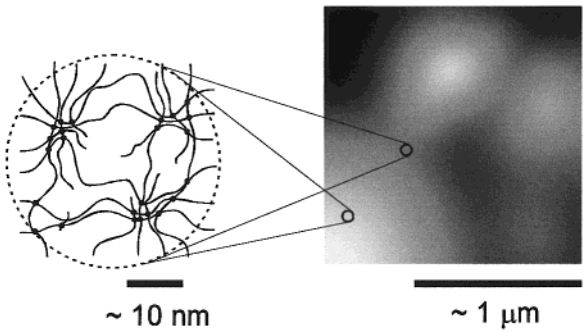

Figure 9. Schematic illustration for the inhomogeneous structure of the polymer network. The PMMA network has the structural hierarchy. On the molecular scale, the network chain forms a microcluster. The inhomogeneous structure in a submicron scale observed in SNOM images was induced by the heterogeneous connection of the microclusters.

was more than 10 times concentrated compared to the ensemble average concentration. Thus, it was found that the local segment density was much larger than the ensemble average density, and the estimated density was almost independent of the probe position through the time-resolved measurement for the local area, whereas the structure appeared heterogeneous in the fluorescence SNOM image. These results indicate that the PMMA network has a structural hierarchy as schematically illustrated in Figure 9. On the molecular scale, the network chain forms a microcluster, in which the chain segment is locally concentrated due to the introduction of cross-linking. Such cross-linked clusters are connected to each other and form the inhomogeneous structure in a length scale of several hundred nanometers, which was observed in the fluorescence SNOM image.

Conclusion

The structural inhomogeneity of the PMMA network was studied by scanning near-field optical microscopy (SNOM). The spatial distribution of network chain segments and cross-links could be directly imaged for optically transparent gels with a high resolution beyond the diffraction limit of light. SNOM allowed us to apply the energy transfer method to a nanometric local area. The energy transfer dynamics through the near-field time-resolved fluorescence technique indicated that the local segment density was higher than the ensemble average density of the network. The local density was independent of the heterogeneous structure in a submicron scale imaged by SNOM. This result indicates that the PMMA network has a hierarchical structure.

Acknowledgment. We thank Prof. Takeji Hashimoto and Prof. Hirokazu Hasegawa, Graduate School of Engineering, Kyoto University, for the use of the ultramicrotome. We thank Prof. Fumihiko Tanaka and Dr. Tsuyoshi Koga, Graduate School of Engineering, Kyoto University, for helpful discussions. This work was supported by a Grant-in-Aid (No. 10875197 and 12305061) from the Ministry of Education, Science, Sports, and Culture of Japan. H.A. acknowledges Research Fellowships of the Japan Society for the Promotion of Science for Young Scientists.

References and Notes

(1) Hsu, T. P.; Ma, D. S.; Cohen, C. *Polymer* **1983**, *24*, 1273.
(2) Weiss, N.; van Vliet, T.; Silberberg, A. *J. Polym. Sci., Polym. Phys. Ed.* **1979**, *17*, 2229.
(3) Hecht, A. M.; Duplessix, R.; Geissler, E. *Macromolecules* **1985**, *18*, 2167.
(4) Mallam, S.; Horkay, F.; Hecht, A. M.; Geissler, E. *Macromolecules* **1989**, *22*, 3356.
(5) Sato-Matsuo, E.; Orkisz, M.; Sun, S.-T.; Li, Y.; Tanaka, T. *Macromolecules* **1994**, *27*, 6791.
(6) Shibayama, M.; Norisuye, T.; Nomura, S. *Macromolecules* **1996**, *29*, 8746.
(7) Ikkai, F.; Shibayama, M. *Phys. Rev. E* **1997**, *56*, 51.
(8) Shibayama, M.; Ikkai, F.; Shiwa, Y.; Rabin, Y. *J. Chem. Phys.* **1997**, *107*, 5227.
(9) Ikkai, F.; Shibayama, M.; Han, C. C. *Macromolecules* **1998**, *31*, 3275.
(10) Rabin, Y.; Panyukov, S. *Macromolecules* **1997**, *30*, 301.
(11) Suzuki, A.; Yamazaki, M.; Kobiki, Y. *J. Chem. Phys.* **1996**, *104*, 1751.
(12) Suzuki, A.; Yamazaki, M.; Kobiki, Y.; Suzuki, H. *Macromolecules* **1997**, *30*, 2350.
(13) Hirokawa, Y.; Jinnai, H.; Nishikawa, Y.; Okamoto, T.; Hashimoto, T. *Macromolecules* **1999**, *32*, 7093.
(14) Ohmori, S.; Ito, S.; Yamamoto, M. *Macromolecules* **1991**, *24*, 2377.
(15) Mabuchi, M.; Kawano, K.; Ito, S.; Yamamoto, M.; Takahashi, M.; Masuda, T. *Macromolecules* **1998**, *31*, 6083.
(16) Aoki, H.; Horinaka, J.; Ito, S.; Yamamoto, M. *Polym. Bull.* **1997**, *37*, 109.
(17) Stein, A. D.; Hoffman, D. A.; Frank, C. W.; Fayer, M. D. *J. Phys. Chem.* **1992**, *96*, 3269.
(18) Farinha, J. P. S.; Martinho, J. M. G.; Kawaguchi, S.; Yekta, A.; Winnik, M. A. *J. Phys. Chem.* **1996**, *100*, 12552.
(19) Tcherkasskaya, O.; Ni, S.; Winnik, M. A. *Macromolecules* **1996**, *29*, 610.
(20) Betzig, E.; Trautman, J. K. *Science* **1992**, *257*, 189.
(21) Vanden Bout, D. A.; Kerimo, J.; Higgins, D. A.; Barbara, P. F. *Acc. Chem. Res.* **1997**, *30*, 204.
(22) Aoki, H.; Sakurai, Y.; Ito, S.; Nakagawa, T. *J. Phys. Chem. B* **1999**, *103*, 10553.
(23) Dutta, A. K.; Vanoppen, P.; Jeuris, K.; Grim, P. C. M.; Pevenage, D.; Salesse, C.; De Schryver, F. C. *Langmuir* **1999**, *15*, 607.
(24) Dunn, R. C. *Chem. Rev.* **1999**, *99*, 2891.
(25) Hecht, B.; Sick, B.; Wild, U. P.; Deckert, V.; Zenobi, R.; Martin, O. J. F.; Pohl, D. W. *J. Chem. Phys.* **2000**, *112*, 7761.
(26) McNeill, J. D.; O'Connor, D. B.; Barbara, P. F. *J. Chem. Phys.* **2000**, *112*, 7811.
(27) van Hulst, N. F.; Veerman, J. A.; Garcia-Parajo, M. F.; Kuipers, L. *J. Chem. Phys.* **2000**, *112*, 7799.
(28) Krakovyak, M. G.; Ananieva, T. D.; Skorokhodov, S. S. *Synth. Commun.* **1977**, *7*, 397.
(29) Ohtsu, M. *Near-Field Nano/Atom Optics and Technology*; Springer: Tokyo, 1998.
(30) Mononobe, S.; Saiki, T.; Suzuki, T.; Koshihara, S.; Ohtsu, M. *Opt. Commun.* **1998**, *146*, 45.

(31) O'Cornner, D. V.; Phillips, D. *Time-Correlated Single Photon Counting*; Academic Press: London, 1984.
(32) Hecht, B.; Bielefeldt, H.; Inouye, Y.; Pohl, D. W.; Novotny, L. *J. Appl. Phys.* **1997**, *81*, 2492.
(33) Hauser, M.; Klein, U. K. A.; Gosele, U. *Z. Phys. Chem. (Munich)* **1976**, *101*, 255.
(34) A toluene solution of PMMA was prepared. The concentration was several percent by weight. Perylene and eosin monomer compounds were dissolved in the PMMA solution. The resulting solution was spin-cast on a cover glass. The near-field time-resolved measurements were carried out in the same manner as the case of the network samples.
(35) Ambrose, W. P.; Goodwin, P. M.; Martin, J. C.; Keller, R. A. *Science* **1994**, *265*, 364.
(36) Xie, X. S.; Dunn, R. C. *Science* **1994**, *265*, 361.
(37) Bian, R. X.; Dunn, R. C.; Xie, X. S. *Phys. Rev. Lett.* **1995**, *75*, 4772.

MA001274+